

# Injectable Magnesium-Enriched Hydroxyapatite Putty in Peri-Implant Defects: A Histomorphometric Analysis in Pigs

Roberto Crespi, MD, MS<sup>1</sup>/Paolo Capparè, MD<sup>2</sup>/Alessandro Addis, DVM<sup>3</sup>/Enrico Gherlone, MD, DMD, PhD<sup>4</sup>

**Purpose:** The purpose of this study was to evaluate the healing of an injectable mixture of nanoparticles of magnesium-enriched hydroxyapatite (mHA) in peri-implant defects. **Materials and Methods:** Thirty-two dental implants were placed in 16 tibiae of eight female Large White pigs. In each animal, four implant beds (two sites each tibia) with medial three-wall intrabony defects were prepared. Via random selection, one bone defect in each tibia was filled with injectable mHA putty ( $n = 16$ , test group), whereas the other defect was not filled ( $n = 16$ , control group). Two animals were sacrificed after 2 weeks, two after 4 weeks, two after 6 weeks, and two after 8 weeks. In all, 32 block section samples were obtained for histologic and histomorphometric analyses. **Results:** The test group exhibited statistically significantly higher values for bone-to-implant contact (BIC) and lower amounts of connective tissue (CT) over time. The test group showed a remarkable increase in vital bone values between 6 and 8 weeks after implant placement. After 8 weeks, the injectable mHA was almost completely resorbed. **Conclusions:** Injectable mHA putty could be a useful and suitable bone grafting material in peri-implant defects. INT J ORAL MAXILLOFAC IMPLANTS 2012;27:95–101

**Key words:** animal study, bone graft, hydroxyapatite, magnesium-enriched hydroxyapatite, peri-implant defect

Peri-implant gaps are the most common type of bone defect associated with placement of an implant in a fresh extraction socket<sup>1</sup> and in manifestations of peri-implantitis.<sup>2</sup> The increasing trend toward implant placement immediately after extraction<sup>3–7</sup> makes problems associated with peri-implant bone defects more likely because of the incongruity of extraction socket walls and implant walls; such sites may require a bone graft to fill the defect gap.

Bone dehiscence resulting from peri-implantitis, overheating of bone during surgical procedures, and a low volume of native bone may be treated by several procedures, but they do not address bone regeneration. Guided bone regeneration procedures can treat bone defects adjacent to dental implants,<sup>8</sup> but membrane exposure and subsequent bacterial colonization can lead to treatment failure.<sup>9</sup>

To preserve alveolar bone and avoid invasive ridge augmentation procedures, several biomaterials have been advocated immediately following tooth extraction to ensure the formation of alveolar bone within implant sites. Bone allograft, bone autograft, and xenografts<sup>10</sup> have all been proposed to maintain bone volume of the alveoli. Because of their biocompatibility and bioactivity, hydroxyapatite (HA) ceramics are commonly used in bone grafting and dental devices as bone substitutes,<sup>11,12</sup> since they have the ability to induce mesenchymal cells to differentiate into osteoblasts; this capacity means that HA ceramics are a potential scaffold material for bone tissue engineering.<sup>13,14</sup> Furthermore, animal and human studies of block, granulated, and powdered forms of calcium phosphate ceramics have proven their efficacy as bone substitute materials for the repair of bone defects.<sup>15,16</sup>

Histologic studies of the healing response to these graft materials with respect to the implant-biomaterial interface and defect filling are mandatory for clinicians to build a scientific basis for selection of the most suitable grafting material(s) for the resolution of defects around implants. The purpose of this study, therefore, was to evaluate histologically the healing during the first 8 weeks following injection of a mixture of nanoparticles of magnesium-enriched hydroxyapatite (mHA) placed in peri-implant bone defects in an animal model.

<sup>1</sup>Clinical Professor, Department of Dentistry, Vita Salute University, San Raffaele Hospital, Milan, Italy.

<sup>2</sup>Clinician, Department of Dentistry, Vita Salute University, San Raffaele Hospital, Milan, Italy.

<sup>3</sup>Private practice, Laboratory Animal Science Lazzaro Spallanzani, Milan, Italy.

<sup>4</sup>Full Professor and Chairman, Department of Dentistry, Vita Salute University, San Raffaele Hospital, Milan, Italy.

**Correspondence to:** Dr Roberto Crespi, Department of Dentistry, Vita Salute University, San Raffaele Hospital, Via Olgettina No. 48, 20123 Milano, Italy. Email: robresp@libero.it

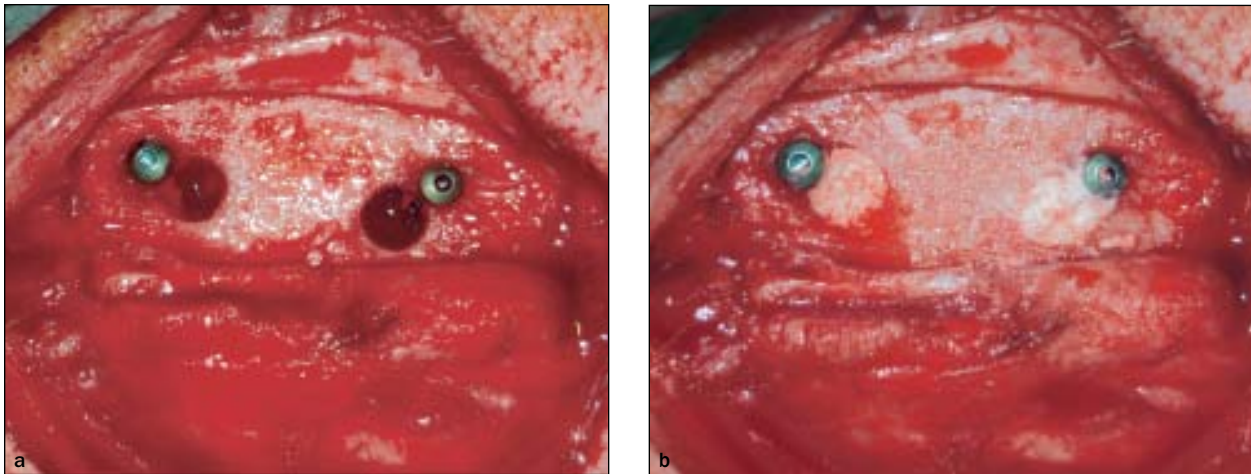


**Fig 1** (a) Implants and defects. The 5-mm-diameter defects were created on the medial of each implant site with a trephine bur. (b) MHA graft in place in the defects.

## MATERIALS AND METHODS

### Animals

Eight female Large White pigs, about 5 months old and weighing on average 70 kg ( $70 \pm 4$  kg), were used. All animals were treated in accordance with the policies and principles of laboratory animal care and with the European Union guidelines (86/609/EEC) approved by the Italian Ministry of Health (Law 116/92).

Pigs were housed separately in standard boxes in temperature-controlled rooms ( $15^{\circ}\text{C}$  to  $20^{\circ}\text{C}$ ) and were allowed to move freely within their boxes. They underwent an adaptation and observation period for 1 week prior to surgery, during which they were fed twice daily with a standard commercial pig diet. Prior to surgery, the pigs fasted overnight, but they were allowed free access to water.

### Surgical Treatment

For all procedures, heavy sedation was first obtained by intramuscular administration of ketamine (10 mg/kg) and midazolam (0.5 mg/kg). Anesthesia was obtained via an oronasal mask with a mixture of isoflurane 4% and oxygen and maintained through intubation with the same gas mixture (isoflurane 3.5%). Intraoperative analgesia was provided with tramadol (1 mg/kg intravenously) plus meloxicam (0.4 mg/kg). To prevent infection, the animals received marbofloxacin (2 mg/kg intravenously) and long-acting amoxicillin (15 mg/kg intramuscularly) at the time of surgery.

The legs were shaved, washed, and decontaminated with a povidone-iodine scrub prior to surgical draping. The proximal tibial metaphysis was surgically exposed via a skin incision and the muscles were dissected to allow elevation of the periosteum using sterile surgical

techniques. In each animal, four implant beds (two sites in each tibia) were prepared with a medial three-walled intrabony defect. Two implants (Winsix) were placed in each tibia. By random selection, the medial bone defect was filled with injectable mHA putty (SintLife Putty, Finceramica) (test group), while the other defect was not filled (control group). The injectable mHA putty (SintLife Putty, Finceramica) used in this study is a novel malleable bone paste made up of nanoparticles and 450- to 900- $\mu\text{m}$  granules of mHA in phosphate-buffered saline solution; its chemical (composition) and chemical-physical (crystallinity) properties correspond to those of human bone matrix. In total, 32 implants were placed (16 in the test group and 16 in the control group).

The implant sites were prepared following the Brånemark protocol (Nobel Biocare). A series of drills with increasing diameters were used under profuse irrigation with sterile saline. Before implant placement, a standardized three-wall intrabony defect ( $5 \times 5 \times 5$  mm) was created at the medial of each intended implant site with a 5-mm-diameter trephine bur (Fig 1a). The bone on the distal side of each implant was left intact.

Dental implants (Winsix), 3.3 mm in diameter and 15 mm in length with a sandblasted surface, were positioned such that the coronal-most portion of the implant body was level with the osseous crest. The implants were placed after threading with a screw tap, with the head on top of the cortex. All implants achieved good primary stability following insertion. For the 16 experimental implants, the injectable mHA was spread by a syringe into the three-wall defect sites; in the 16 control sites, the bone defects were unfilled. Excess putty was removed and the remaining material was shaped to the geometry of the defect (Fig 1b). The

soft tissues were reapproximated and closed with 4-0 resorbable sutures. The fascia and skin were sutured in separate layers with resorbable sutures.

Postoperatively, the animals were given meloxicam (0.4 mg/kg intramuscularly) and enrofloxacin (5 mg/kg intramuscularly) once a day for the following 4 days.

Two animals were sacrificed after 2 weeks of healing, two animals after 4 weeks, two after 6 weeks, and two after 8 weeks with an intravenous overdose of potassium chloride after they had been anesthetized as described previously.

### Histologic Preparation

The tibiae were block-resected with an oscillating autopsy saw. The recovered segments with implants were preserved and fixed for 7 days in 4% buffered paraformaldehyde, dehydrated in a graded series of alcohols (24 hours each in 50%, 75%, 95%, and 100%), and embedded in methyl methacrylate (Merck Schuchardt).

The samples were cleaned of all soft tissue; then they were fixed in Karnovsky's fixative and dehydrated in a graded series of alcohols for undecalcified bone processing in glycol methyl methacrylate. Blocks were sectioned along the sagittal plane, perpendicular to the implant's major axis, and cut with a 1600 machinery cutter (Leica Microsystem). Three sections per implant were obtained in a longitudinal direction, parallel to the implant axis.

Sections, each 15  $\mu\text{m}$  thick, were obtained and stained with Goldner trichrome (modification). The sections were placed in Weigert hematoxylin, washed in tap water, and differentiated with 0.5% acid alcohol. Next, they were stained in Ponceau/acid fuchsin/azophloxine and counterstained with phosphomolybdic acid/orange G and light green (so that nuclei would appear blue-black, osteoid and collagen fibers would appear red, and mineralized bone would stain green). Histologic samples were observed with a FOMI III microscope by Normasky differential interference contrast (Fomi III, Carl Zeiss).

### Histomorphometric Analysis

Measurements were made in the area of the previous bone defect outside the implant threads.<sup>17</sup> For each defect site, the percentages of bone-to-implant contact (BIC), vital bone (VB), connective tissue (CT), and residual graft material (RGM) were recorded using histomorphometric analysis and were evaluated. BIC was defined as the percentage of the length of the region in which bone is directly opposed to the implant without the presence of fibrous tissue. All measurements were repeated for test and control sites, and the presented data were based on the average of the three measured sections.

For measurement of the bone-regenerative efficacy of the mHA injectable putty in the bone defects, each section was examined at a magnification of 10 $\times$  with a light microscope (Axioskope, Carl Zeiss) connected to a digital camera (Leica DC 280, Leica Microsystem), and a software program (Alexasoft Image Pro Plus 2.5, Microcontrol) was used to evaluate and calculate the histomorphometric parameters.

### Statistical Analysis

Dedicated software was used for all statistical analyses (SPSS version 11.5.0, IBM). All values were presented as means  $\pm$  standard deviations. Comparisons between test and control groups were performed with the Student *t* test ( $P < .05$  was considered the threshold for statistical significance).

## RESULTS

Postoperative healing at different intervals following implant placement was uneventful in all pigs. Radiologic examination revealed no pathologic processes around implants.

### Histologic Findings

All implants were osseointegrated, and there was no sign of inflammatory response. After 2 weeks it was possible to observe osteoid matrix between the implant surface and the mHA particles, showing the good osteogenic potential of the bone substitute. New bone formation began just after surgery, since osteoid lamellae were present between the implant surface and the mHA granules. In comparison, no lamellar formation was observed after 2 weeks in unfilled defects (Figs 2a to 2c).

After 4 weeks, osteogenic activity could be seen originating from the bottom and the walls of the defect, and an osteoid deposition matrix surrounded the mHA granules and implant surfaces (Fig 2d). At that time osteoclastlike cells were seen in resorption lacunae, providing evidence that the biomaterial was being actively replaced by new bone. Osseointegration and remodeling processes could be observed along the bone-implant interface in both test and control sections.

After 6 weeks, the mHA was in direct contact with the host bone in all sections, and woven bone tissue was in contact with the implant surface (Fig 2e). After 8 weeks, the mHA in the defect sites had been replaced by new bone and new osteons were seen (Fig 2f). A lamellar pattern, stained in green, revealed bone apposition along the implant surface and the resorption of mHA granules by macrophagic activity. In test group specimens at 8 weeks, more lamellar bone apposition was observed than in the control specimens, where more medullary tissue rich in fat cells was seen (Fig 2g).

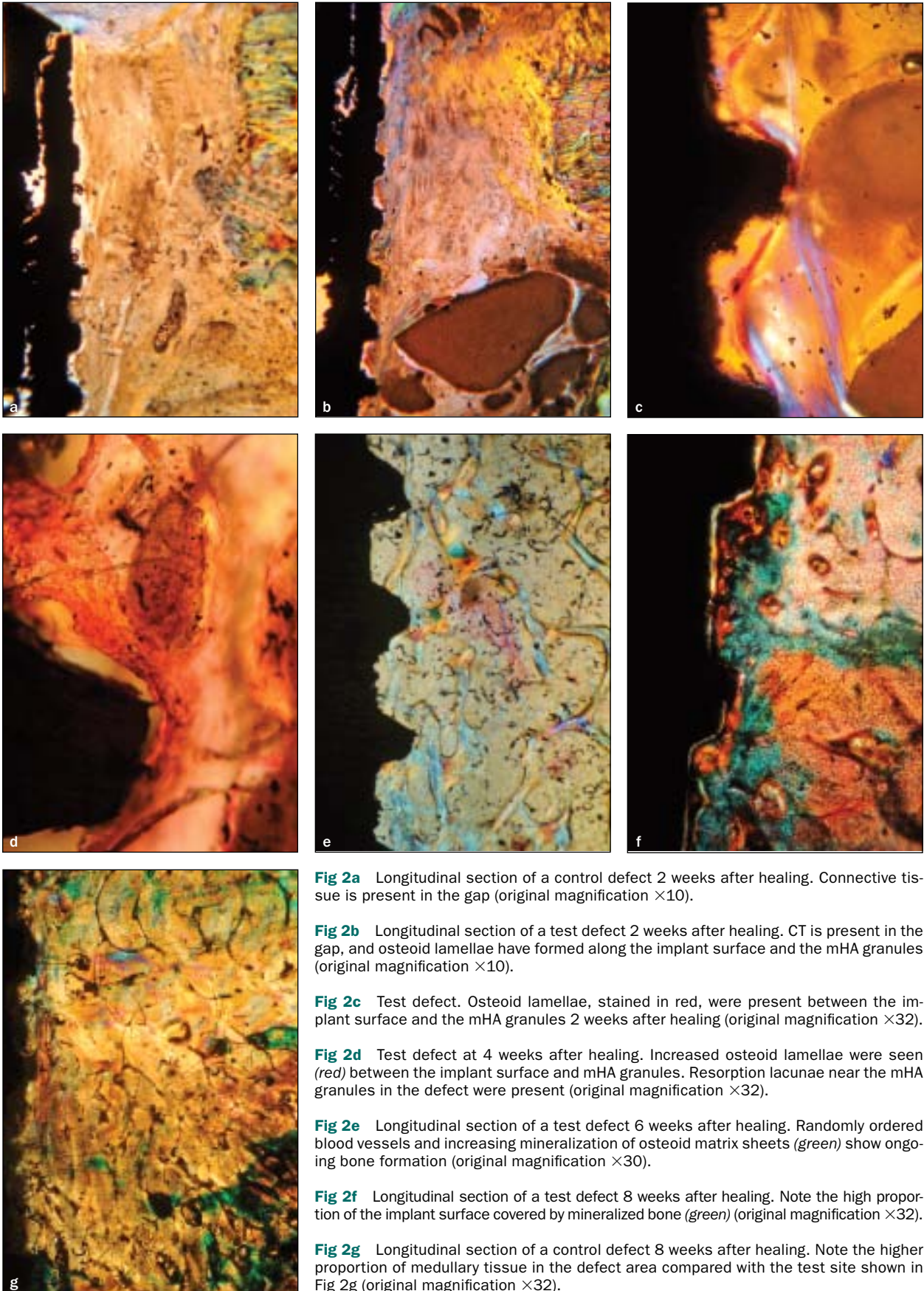


**Fig 2a** Longitudinal section of a control defect 2 weeks after healing. Connective tissue is present in the gap (original magnification  $\times 10$ ).

**Fig 2b** Longitudinal section of a test defect 2 weeks after healing. CT is present in the gap, and osteoid lamellae have formed along the implant surface and the mHA granules (original magnification  $\times 10$ ).

**Fig 2c** Test defect. Osteoid lamellae, stained in red, were present between the implant surface and the mHA granules 2 weeks after healing (original magnification  $\times 32$ ).

**Fig 2d** Test defect at 4 weeks after healing. Increased osteoid lamellae were seen (red) between the implant surface and mHA granules. Resorption lacunae near the mHA granules in the defect were present (original magnification  $\times 32$ ).

**Fig 2e** Longitudinal section of a test defect 6 weeks after healing. Randomly ordered blood vessels and increasing mineralization of osteoid matrix sheets (green) show ongoing bone formation (original magnification  $\times 30$ ).

**Fig 2f** Longitudinal section of a test defect 8 weeks after healing. Note the high proportion of the implant surface covered by mineralized bone (green) (original magnification  $\times 32$ ).

**Fig 2g** Longitudinal section of a control defect 8 weeks after healing. Note the higher proportion of medullary tissue in the defect area compared with the test site shown in Fig 2g (original magnification  $\times 32$ ).

**Table 1 Histomorphometric Results 2 Weeks After Implant Placement**

Parameter	Test (n = 4)	Control (n = 4)
BIC (%)	44.1 ± 11.9*	18.7 ± 7.0*
VB (%)	27.4 ± 11.9	44.1 ± 11.9
CT (%)	17.7 ± 6.3*	61.2 ± 8.1*
RGM (%)	63.2 ± 11.1	–

\*Statistically significant difference between test and control groups ( $P < .05$ ).

**Table 2 Histomorphometric Results 4 Weeks After Implant Placement**

Parameter	Test (n = 4)	Control (n = 4)
BIC (%)	47.3 ± 11.3*	27.0 ± 5.9*
VB (%)	28.8 ± 10.5	36.1 ± 11.3
CT (%)	23.3 ± 5.6*	58.6 ± 9.2*
RGM (%)	50.1 ± 8.4	–

\*Statistically significant difference between test and control groups ( $P < .05$ ).

**Table 3 Histomorphometric Results 6 Weeks After Implant Placement**

Parameter	Test (n = 4)	Control (n = 4)
BIC (%)	49.9 ± 8.4*	31.9 ± 6.7*
VB (%)	30.0 ± 9.7	36.8 ± 10.7
CT (%)	23.8 ± 7.0*	61.2 ± 10.1*
RGM (%)	49.8 ± 9.1	–

\*Statistically significant difference between test and control groups ( $P < .05$ ).

**Table 4 Histomorphometric Results 8 Weeks After Implant Placement**

Parameter	Test (n = 4)	Control (n = 4)
BIC (%)	57.2 ± 6.9*	40.8 ± 7.8*
VB (%)	65.1 ± 11.2*	42.3 ± 9.5*
CT (%)	29.0 ± 7.9*	64.5 ± 10.6*
RGM (%)	6.2 ± 5.1	–

\*Statistically significant difference between test and control groups ( $P < .05$ ).

These observations provide evidence that mHA served as a good scaffold for new bone regeneration, maintaining the volume of the defect and allowing the bone to mineralize around the implant surface.

### Histomorphometric Observations

The recorded histomorphometric values in test and control sites are reported in Tables 1 to 4.

In sections obtained from pigs sacrificed after 2 weeks (Table 1), test sites demonstrated statistically significantly higher mean BIC values than control sites. At the same time, test group samples presented statistically significantly lower values for CT than control group samples. No statistically significant differences were found for VB. RGM was  $63.2\% \pm 11.1\%$ .

In sections obtained from pigs sacrificed after 4 and 6 weeks (Tables 2 and 3, respectively), a similar trend was observed. The test group demonstrated a statistically higher mean BIC value than the control group, along with statistically significant lower CT values than the control group at both time points. No statistically significant differences were found for VB.

At 8 weeks after implant placement (Table 4), the test group again demonstrated statistically significantly greater mean BIC values than the control group ( $57.2\% \pm 6.9\%$  versus  $40.8\% \pm 7.8\%$ , respectively) and statistically significantly lower values for CT than the control group ( $29.0\% \pm 7.9\%$  versus  $64.5\% \pm 10.6\%$ ). At this time point, statistically significant differences were found for VB: the test group reported a significantly

higher value than the control group ( $65.1\% \pm 11.2\%$  versus  $42.3\% \pm 9.5\%$ ). Residual graft material was  $6.2\% \pm 5.1\%$ .

Overall, the test group reported consistently higher values for BIC and lower values for CT. In addition, between 6 and 8 weeks after implant placement, test sites showed a remarkable increase in VB. After 8 weeks, the graft material had been almost completely resorbed.

### DISCUSSION

In the present study, oral implants were placed in pig tibiae to evaluate the effect of placement of an injectable mHA putty in a peri-implant dehiscence model, since the pig features bone remodeling processes that are similar to those of humans, comprising both trabecular and intracortical basic multicellular unit-based remodeling.<sup>18,19</sup> A study of the effects of fluoride on cortical bone remodeling in growing pigs showed that these animals have a cortical bone mineralization rate that is similar to that of humans.<sup>20</sup> Therefore, pig tibiae seem to be suitable for evaluation of a peri-implant bone defect, as this site features abundant bone volume. The animals were sacrificed every 2 weeks to evaluate the deposition of osteoid matrix, the formation of lamellar bone between the implant surface and the biomaterial granules, and the timing of the resorption of injectable mHA putty.

The current study demonstrated a beneficial effect on bone formation and mineralization following the addition of injectable mHA putty to the bone defects, since osteoid lamellar bone was present after only 2 weeks between the implant surface and the mHA granules. In comparison, no lamellar formation was observed at 2 weeks in the unfilled defects. The osteoid matrix was successively substituted by lamellar bone around the implant surfaces, resulting in a high percentage of BIC.

No foreign-body reactions or inflammatory responses were observed histologically around the injectable mHA putty used in this study. Only small circular zones of the biomaterial remained in direct contact with new bone tissue after 8 weeks. Furthermore, after 8 weeks of healing, no injectable mHA particles were observed in contact with the implant surface, showing favorable biodegradation and substitution because of the chemical composition and micromorphometry of the biomaterial.

These histologic and histomorphometric results may be explained better by a study in humans in which mHA and autogenous bone graft for maxillary sinus elevation were compared.<sup>21</sup> Gene expression analyses indicated that primary osteoblasts from mHA-grafted samples displayed enhanced expression of the osteoblast-specific differentiation factor *Cbfa1* and osteocalcin, a marker of matrix-forming activity. Moreover, osteoblasts from the biomaterial-engrafted sites revealed a marked decrease in receptor activator of nuclear factor kappa B ligand (RANKL) expression, with comparable levels of osteoprotegerin, thus revealing a decreased RANKL/osteoprotegerin ratio; this may explain the decreased osteoclast differentiation and activity and the comparable bone volume yield in the two groups. Together, the data are compatible with a higher bone-forming activity coupled with reduced osteoclastogenic activity and decreased bone resorption, and they may explain why similar percentages of total BV are generated by biomaterial grafts, despite higher percentages of nonvital bone (containing osteocytic lacunae) and lower VB. The simultaneous evaluation of osteoblast-specific factors involved in matrix deposition, together with the ratio between the crucial osteoblast-related pro- and anti-osteoclastogenic factors RANKL and osteoprotegerin, could enable a determination not only of the activity of osteoblasts as matrix secretors, but also the cross-talk between osteoblastic cells with nascent and active osteoclasts. The present study strongly suggests that analysis of the gene expression profiles of primary osteoblasts would be useful to determine whether a given biomaterial possesses not only direct osteoconductive but also indirect osteoinductive effects.

The histologic findings reported in the present study and gene expression values explained previ-

ously may help clarify the results of a clinical study that evaluated radiographic parameters of implants positioned in grafted alveoli with three different biomaterials: mHA, calcium sulfate, and heterologous porcine bone.<sup>22</sup> The aim of the study was to evaluate the clinical outcome of implants placed in previously grafted alveoli and expanded at stage-two surgery by the osteotome technique.<sup>23</sup> The study showed that after 2 and 3 years, the success of implants placed in grafted sockets was not influenced by the biomaterial used, since no negative impacts were seen on the clinical outcome.

Human studies<sup>24–26</sup> have reported encouraging histomorphometric data about porous HA as a sinus grafting material, as revealed by light microscopy and transmission electron microscopy. In most cases, the biomaterial particles remained in close contact with bone, which appeared compact, with well-organized lamellae. A cementlike line was barely visible at the bone-biomaterial interface, but there were no gaps or interposed connective tissue in between. Histology and histomorphometry showed that the incompletely resorbed HA graft was well integrated into the biopsy specimens and in complete continuity with the newly formed bone.

Arisan et al<sup>27</sup> applied an injectable calcium phosphate cement to standardized buccal dehiscence peri-implant defects after implant site preparation in the right proximal tibiae of five beagle dogs. Healing was uneventful in all dogs. The injectable calcium phosphate putty showed good space maintenance and osteoconductive properties and did not provoke any foreign-body reactions. BIC was 34.42% ( $\pm$  19.88%) and 37.00% ( $\pm$  21.33%) ( $P = .375$ ), while LBH was 84.23% ( $\pm$  19.73%) and 96.10% ( $\pm$  6.66%) ( $P = .125$ ) for test and control sites, respectively. In another study,<sup>28</sup> the healing of different bone grafting materials adjacent to titanium plasma-sprayed endosseous dental implants was investigated. The results indicated that percent BIC and percent bone height fill in intrabony defects around titanium plasma-sprayed implants were statistically significantly higher with the use of demineralized freeze-dried bone allograft in comparison to control defects that were left unfilled.

## CONCLUSIONS

Within the limits of the present animal study, injectable mHA putty could be considered a useful and suitable bone grafting material for peri-implant defects. Further studies are needed to evaluate this biomaterial in humans.

## ACKNOWLEDGMENTS

The authors are grateful to Dr Elisabetta Mariani and BoNetwork (San Raffaele Scientific Institute, Milan, Italy) for preparation of the histologic samples.

## REFERENCES

- Mellonig JT, Nevins M. Guided bone regeneration of bone defects associated with implants: An evidence based outcome assessment. *Int J Periodontics Restorative Dent* 1995;15:168–185.
- Hammerle CH, Karing T. Guided bone regeneration at oral implant sites. *Periodontol* 2000 1998;17:151–175.
- Tolman D, Keller E. Endosseous implant placement immediately following dental extraction and alveoloplasty: Preliminary report with 6-year follow-up. *Int J Oral Maxillofac Implants* 1991;6:24–28.
- Wilson TG, Schenk R, Buser D, Cochran D. Implants placed in immediate extraction sites: A report of histologic and histometric analyses of human biopsies. *Int J Oral Maxillofac Implants* 1998;13:333–341.
- Cornelini R, Cangini F, Covani U, Wilson T. Immediate restoration of implants placed into fresh extraction sockets for single-tooth replacement: A prospective clinical study. *Int J Periodontics Restorative Dent* 2005;25:439–447.
- Barone A, Rispoli L, Vozza I, Quaranta A, Covani U. Immediate restoration of single implants placed immediately after tooth extraction. *J Periodontol* 2006;77:1914–1920.
- Crespi R, Cappare P, Gherlone E, Romanos GE. Immediate occlusal loading of implants placed in fresh sockets after tooth extraction. *Int J Oral Maxillofac Implants* 2007;22:955–962.
- Becker W, Dahlin C, Becker B, et al. The use of e-PTFE barrier membranes for bone promotion around titanium implants placed into extraction sockets: A prospective multicenter study. *Int J Oral Maxillofac Implants* 1994;9:31–40.
- Chiapasco M, Zaniboni M, Boisco M. A prospective clinical study of bone augmentation techniques at immediate implants. *Clin Oral Implants Res* 2005;2:176–184.
- Artzi Z, Tal H, Dayan D. Porous bovine bone mineral in healing of human extraction sockets. Part I. Histomorphometric evaluation at 9 months. *J Periodontol* 2000;71:1015–1023.
- Ripamonti U. The morphogenesis of bone in replicas of porous HA obtained from conversion of calcium carbonate exoskeletons of coral. *J Bone Joint Surg* 1991;73A:692–703.
- Yuan H, Li Y, Yang Z, Feng J, Zhang XD. An investigation on the osteoinduction of synthetic porous phase-pure HA ceramics. *Biomed Eng Appl Basis Com* 1997;9:274–278.
- Okumura M, Ohgushi H, Dohi Y, et al. Osteoblastic phenotype expression on the surface of HA ceramics. *J Biomed Mater Res* 1997;37:122–129.
- Norman ME, Elgandy HM, Shors EC, el-Amin SF, Laurencin CT. An in-vitro evaluation of coralline porous HA as a scaffold for osteoblast growth. *Clin Mater* 1994;17:85–91.
- Ooms EM, Wolke JG, van der Waerden JP, Jansen JA. Trabecular bone response to injectable calcium phosphate (Ca-P) cement. *J Biomed Mater Res* 2002;1:9–18.
- Fellah BH, Weiss P, Gauthier O. Bone repair using a new injectable self-crosslinkable bone substitute. *J Orthop Res* 2006;4:628–635.
- Sanchez AR, Sheridan PJ, Eckert SE, Weaver AL. Regenerative potential of platelet-rich plasma added to xenogenic bone grafts in peri-implant defects: A histomorphometric analysis in dogs. *J Periodontol* 2005;76:1637–1644.
- Mosekilde L, Kragstrup J, Richards A. Compressive strength, ash weight, and volume of vertebral trabecular bone in experimental fluorosis in pigs. *Calcif Tissue Int* 1987;40:318–322.
- Mosekilde L, Weisbrode SE, Safron JA, et al. Calcium-restricted ovariectomized Sinclair S-1 minipigs: An animal model of osteopenia and trabecular plate perforation. *Bone* 1993;14:379–382.
- Kragstrup J, Richards A, Fejerskov O. Effect of fluoride on cortical bone remodeling in the growing domestic pig. *Bone* 1989;10:421–424.
- Crespi R, Mariani E, Benasciutti E, Cappare P, Cenci S, Gherlone E. Magnesium-enriched hydroxyapatite versus autologous bone in maxillary sinus grafting: Combining histomorphometry with osteoblast gene expression profiles in vivo. *J Periodontol* 2009;80:586–598.
- Crespi R, Cappare P, Gherlone E. Dental implants placed in extraction sites grafted with different bone substitutes: Radiographic evaluation at 24 months. *J Periodontol* 2009;80:1616–1621.
- Crespi R, Cappare P, Gherlone E. Osteotome sinus floor elevation and simultaneous implant placement in grafted biomaterial sockets. 3 years follow-up. *J Periodontol* 2010;81:344–349.
- Mangano C, Scarano A, Iezzi G, et al. Maxillary sinus augmentation using an engineered porous hydroxyapatite: A clinical, histological, and transmission electron microscopy study in man. *J Oral Implantol* 2006; 32:122–131.
- Smeets R, Grosjean MB, Jelitte G, et al. Hydroxyapatite bone substitute (Ostim) in sinus floor elevation. Maxillary sinus floor augmentation: Bone regeneration by means of a nanocrystalline in-phase hydroxyapatite (Ostim) [in French, German]. *Schweiz Monatsschr Zahnmed* 2008;118:203–212.
- Lee YM, Shin SY, Kim JY, Kye SB, Ku Y, Rhyu IC. Bone reaction to bovine hydroxyapatite for maxillary sinus floor augmentation: Histologic results in humans. *Int J Periodontics Restorative Dent* 2006;26:471–481.
- Arisan V, Özdemir T, Anil A, Jansen JA, Özer K. Injectable calcium phosphate cement as a bone-graft material around peri-implant dehiscence defects: A dog study. *Int J Oral Maxillofac Implants* 2008;23:1053–1062.
- Hall E, Meffert RM, Hermann JS, Mellonig JT, Cochran DL. Comparison of bioactive glass to demineralized freeze-dried bone allograft in the treatment of intrabony defects around implants in the canine mandible. *J Periodontol* 1999;70:526–535.